Wavelet analysis of angular distributions of secondary particles in high energy nucleus-nucleus interactions

Irregularity of particle pseudorapidity distributions

V.V.Uzhinskii, V.Sh.Navotny[1], G.A.Ososkov, A.Polanski, M.M.Chernyavski[2]

Joint Institute for Nuclear Research,
Laboratory of Information Technologies

Experimental data on sulphur and oxygen nuclei interactions with photoemulsion nuclei at the energies of 200 and 60 GeV/nucleon are analyzed with the help of a continuous wavelet transform. Irregularities in pseudorapidity distributions of narrow groups of the secondary shower particles in the mentioned interactions are observed at application of the second order derivative of Gaussian as a wavelet. The irregularities can be interpreted as an existence of the preference emission angles of groups of particles. Such an effect is expected at emission of Cherenkov gluons in nucleus-nucleus collisions. Some of the positions of the observed peculiarities on the pseudorapidity axis coincide with those found by I.M.Dremin et al. (I.M.Dremin et al. Phys. Lett., 2001, v. B499, p. 97).)

In the last decade a new type of mathematical analysis of data, the so-called wavelet analysis has become very popular in various branches of science and engineering [1]–[4]. Mainly, it is applied for analysis of time series coming from geophysics, meteorology, astrophysics, and so on (applications in aviation, medicine and biology see in [5]).

The wavelet decomposition or wavelet transform of a function $f(x)$ is its decomposition on an orthogonal functional family of special form [6];

$$W_\Psi(a,b)f = \frac{1}{\sqrt{C_\Psi}} \int_{-\infty}^{\infty} f(x)\Psi_{a,b}(x)dx, \tag{1}$$

$$\Psi_{a,b}(x) \equiv a^{-1/2}\Psi\left(\frac{x-b}{a}\right),$$

where Ψ is called a wavelet, b – a translation parameter, a – a dilation parameter or a scale, and C_Ψ – a normalizing constant

$$C_\Psi = 2\pi \int_{-\infty}^{+\infty} |\tilde{\Psi}(\omega)|^2 |\omega|^{-1} d\omega,$$

where $\tilde{\Psi}(\omega)$ – Fourier transform of $\Psi(x)$.

The derivatives of the Gaussian function are often used as wavelets

$$\Psi(x) \equiv g_n(x) = (-1)^{n+1}\frac{d^n}{dx^n}\mathrm{e}^{-x^2/2}, \quad n > 0, \quad C_{g_n} = 2\pi(n-1)!.$$

The first two wavelets are well known:

$$g_1(x) = -x\mathrm{e}^{-x^2/2}, \quad g_2(x) = (1-x^2)\mathrm{e}^{-x^2/2}.$$

[1]FTI, Tashkent, R. Uzbekistan
[2]FIAN, Moscow, Russia

The second one is called Mexican Hat wavelet (MHAT).

As seen, the wavelet transform puts in correspondence to the function of one variable, $f(x)$, the function of two variables, $W_\Psi(a,b)$. Until recently, a presentation and an analysis of a function of two variables was quite a difficult job, and only modern computers with their 3D-graphics allowed one to implement completely the method of wavelet analysis.

There is a discrete analogy of the continuous wavelet transform (see [6]). It was used in elementary particle physics for the study of events of cosmic rays interactions with materials – at the analysis of particle pseudorapidity distributions [7]. The wavelet coefficients ($W_\Psi(a,b)$) of energy distributions predicted by different models of multi-particle production were studied in [8]. Possibilities of the wavelet analysis in searching for manifestation of the disoriented chiral condensate in the pseudorapidity distributions of neutral particles fraction were considered in [9].

In papers [10] the wavelet transform was used for pattern recognition in $Pb+Pb$-interactions at the energy of 158 GeV/nucleon. Structures were found in the angular distributions of secondary particles that can be interpreted as irradiation of Cherenkov gluons. The last publications in this research are devoted to experimental search for the disoriented chiral condensate in nucleus-nucleus interactions [11].

Most of the mentioned papers suffer from the apparent lack of quantitative results which caused either by uniqueness of nature phenomenon or low statistics of analyzed data. It is connected partly with specific properties of the wavelet analysis itself (see [12]). A regular method of wavelet analysis application in particle physics is needed. Our paper presents experience of using the wavelet transform for analysis of more than 2000 interactions of nuclei with nuclei at high energies.

Experimental data were obtained at horizontal irradiation of NIKFI BR-2 nuclear photoemulsion by sulfur and oxygen nucleus with the energies of 200 and 60 GeV per nucleon at the CERN SPS. The sensitivity of emulsion was about 30 grains per unit length of 100 μm for single charged particles with minimal ionization.

Primary interactions were found by along-the track double scanning: fast in the forward direction and slow in the backward direction. Fast scanning was made with a velocity excluding any discrimination of events in the number of heavily ionizing tracks, slow scanning was carried out to find events, if any, with little changed and unbiased projectile nucleus. Upon rejecting events of electromagnetic dissociation and purely elastic scattering in the total sample, 884 events of $S+Em$ and 504 events of $O+Em$ at the energy of 200 GeV/nucleon, and 884 $O+Em$ interactions at the energy of 60 GeV/nucleon were selected for a further analysis. In each event the polar angles θ and azimuthal angles φ were measured.

Shower particles, or the so-called s-particles – single charged particles with a velocity $\beta = v/c \geq 0.7$, are considered in this study. The s-particles consist mainly of produced particles and single charged nuclear fragments. A special separation of single charged fragments was not done.

According to Ref. [10], a distribution of the secondary particles on the pseudorapidity $\eta = -\ln(\tan(\theta/2))$ in an event was presented as

$$f(\eta) = \frac{dn}{d\eta} = \frac{1}{N}\sum_{i=1}^{N}\delta(\eta-\eta_i), \tag{2}$$

where N is multiplicity of s-particles in the event, and η_i is pseudorapidity of i-th particle.

A wavelet transform of the function (2) gives

$$W_\Psi(a,b) = \frac{1}{N}\sum_{i=1}^{N} a^{-1/2}\Psi\left(\frac{x-b}{a}\right). \qquad (3)$$

So, the function of two variables is brought into correspondence with each particle. Wavelet spectra of the event ($W_\Psi(a,b)$) is a sum of such functions.

As an example, Fig. 1 presents wavelet spectra of event with 6 particles having pseudorapidities $\eta_1 = 1$, $\eta_2 = 2.75$, $\eta_3 = 3.25$, $\eta_4 = 5$, $\eta_5 = 6$, $\eta_6 = 7$. The values of translation parameter b are put on the X-axis, dilation parameter, a – on Y-axis. The values of the wavelet coefficients are depicted in a gray-level scale: the high values of the coefficients are of light shade while the lower ones are darker. As seen, in g_2 wavelet spectra at the scale lower than 0.3 all particles are distinguished. At the scale larger than 0.5, the particles 2 and 3 can not be resolved. At $a > 1$ particles 4, 5, 6 can not be resolved. At $a > 2$ one could expect a fusion of particles 1, 2, and 3. However, this does not take place due to small yield of particle 1 in the wavelet spectra at a large scale. So, the wavelet transform of g_2 allows one to study the particle clusterization.

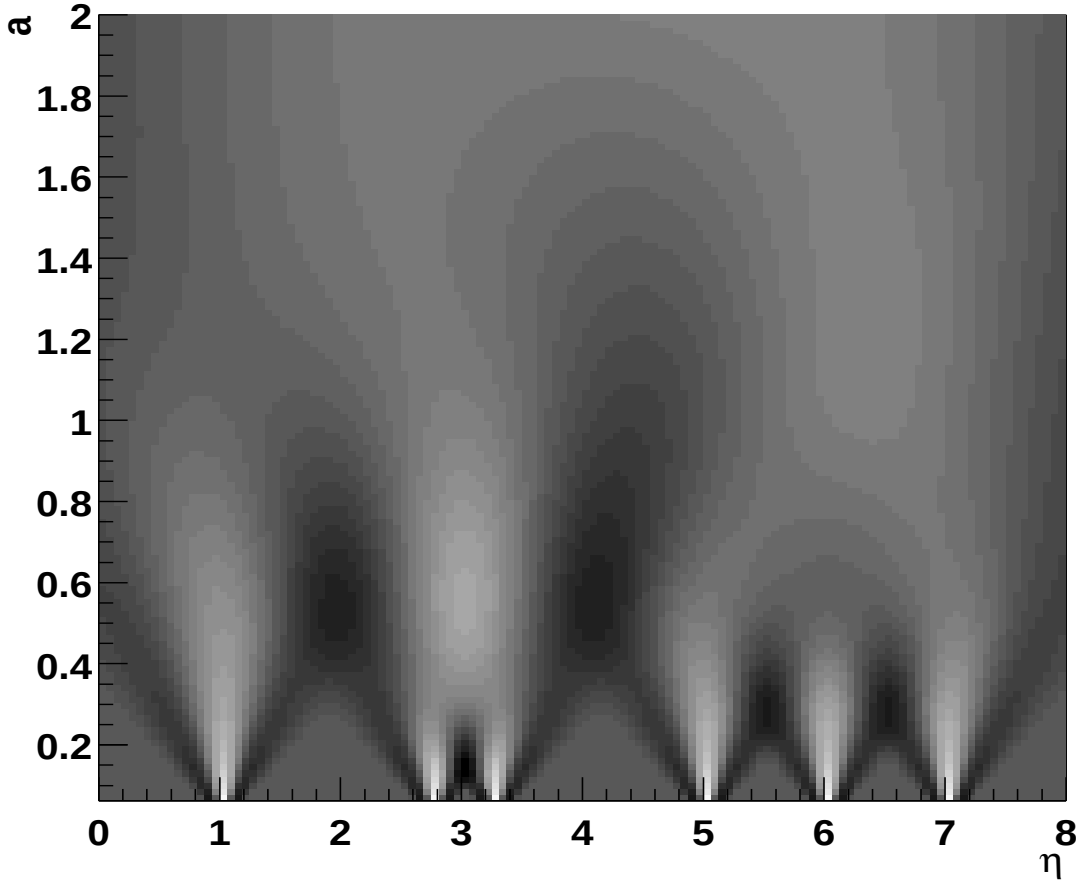

Figure 1: Wavelet spectra, energy densities, and scalogramms

Let us note that the positions of the local maximums of $W_\Psi(a,b)$ ($a \simeq 0.5$ and $b = 3$, $a \simeq 1$ and $b = 6$) on the b-axis are connected with positions of the centers of the groups of particles 2, 3 and 4, 5, 6. The corresponding scales reflect the width of the groups on the pseudorapidity axis. Positions of the local minimums give the centers of the pseudorapidity splits between the groups.

There are a lot of wavelets. Different representations of the 6 particles of the test example are shown in Fig. 1. There are also energy densities ($W_\Psi(a,b)^2$) and scalogramms $E_W(a) = \int W_\Psi(a,b)^2 db$, which are often used in practice.

The g_1 wavelet (see (2)) has a minimum at a negative value of its argument and maximum – at positive value. Positions of these extreme points at different scales can be seen quite well in the energy density spectra. The g_2 wavelet has 3 extreme points. All of them are presented in the energy spectra (see the region of the 1 particle). Scalogramms give generalized imagination of the extreme points.

As seen in the figure, different wavelets give different presentations of particles. The more "usual" ones are obtained at the application of even wavelets. Perhaps, odd wavelets can be useful at automatic data processing.

At the first glance, the g_1 wavelet allows one to locate the regions of unhomogeneouslity in the particle distribution. The positions of the local maxima of the energy spectra on the b-axis ($b = 2.5$ and $b = 3.5$) mark the group of the particles 2 and 3, and the positions on the a-axis show the group size. Though, the following local maxima are disposed at $a = 4$ and $b \sim 0$, $b \sim 9$. There is no selection of the group of the particles 4, 5, 6. At the same time, there are irregularities (extreme points and inflection points) in the corresponding scalogramm which are probably connected with characteristics of the particle group. 7 There are extreme points in the scalogramm obtained with help of the g_2 wavelet at $b \simeq 0.5$ and 1.2 associated with the group characteristics. So, we believe that scalogramms can be used for fast search of the particle group.

The g_4 wavelet has analogous properties. Though, the characteristics of the corresponding scalogramms are not so strongly correlated with the particle characteristics. Thus, below we will use mainly the g_2 wavelet.

We started our analysis with study of the particle distribution on the pseudorapidities in all interactions. The histogrammed distribution for $S + Em$ interactions at the energy of 200 GeV/nucleon is presented in Fig. 2. There are also g_2 and g_4 wavelet spectra at different scales. It should be noted that the wavelet transform was applied to raw experimental data, not to the histogrammed distribution. Thus, a fine structure of the spectra can be observed at small scales. The structure becomes more regular at large scales, and turns to the wavelet function in the limit of large a. At $a \sim 0.4$ one can see 3 maxima in the g_2 spectra at $\eta \sim 2$, 4 and 8. It seems that the maximum at $\eta \sim 2$ is connected with the particle production in the target fragmentation region; the maximum at $\eta \sim 4$ – with the particle production in the central region, and the maximum at $\eta \sim 8$ – with spectator fragments of the projectile nucleus. In reality, the three maxima only reflect what can be seen with the naked eye – the left wing of the distribution is different from the right one. One can clearly see a change of the slope on the right wing at $\eta \sim 6$. At smaller scales the structure is more rich and does not allow such simple interpretation. In order to find selected scales in the interactions and to analyze a fine structure of the events, we turned to a study of the energy density and scalogramm.

The spectrum of the energy density reflects peculiarities of $W_\Psi(a,b)$ function and can be used for searching the particle group. Though, definition of maxima and minima of the

function is a quite complicated task. So, at the first stage we concentrated our attention on the energy distribution on scales, on scalogramm because it is a 1D-function.

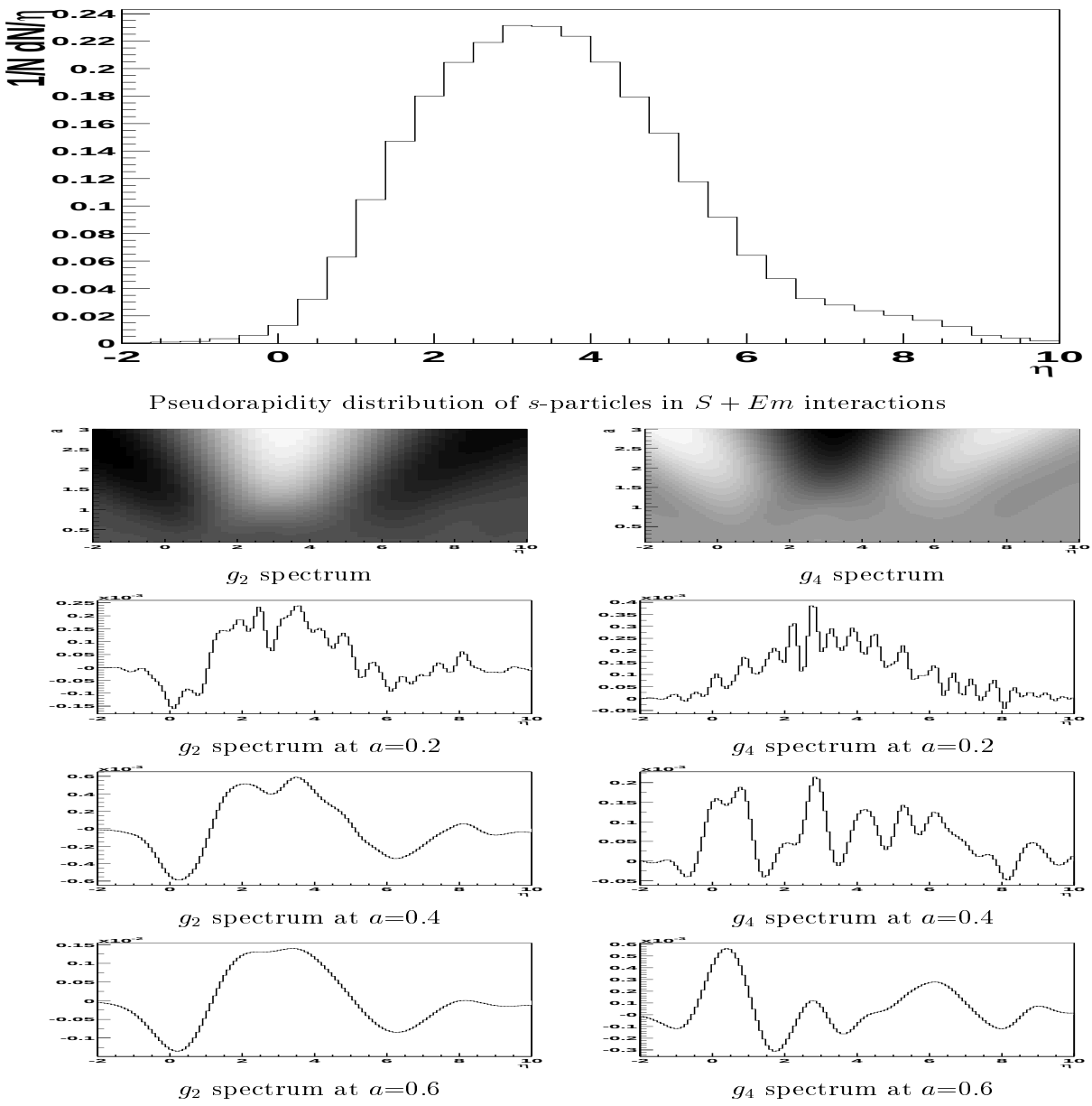

Figure 2: Wavelet analysis of s-particles pseudorapidity distribution in $S + Em$ interactions at the energy 200 GeV/nucleon

Scalogramms reflect characteristic features of events according to the test example. For example, the scalogramm of the g_2 spectrum has the minimum at $a \sim 1.1$ associated with an average distance between the groups of the particles 2, 3 and 4, 5, 6, and the maximum at $a \sim 0.5$, connected with the most compact group of particles 2, 3. It is possible to write out an analytical expression for the scalogramm using the g_2 wavelet

and the distribution of the form (2).

$$S(a) = \frac{1}{32\sqrt{\pi}a^4} \sum_{i,j=1}^{N} \left[\Delta_{i,j}^4 - 12a^2\delta^2 - 12a^4\right] e^{-\frac{\Delta_{ij}^4}{4a^2}} \tag{4}$$

$$\Delta_{ij} = \eta_i - \eta_j$$

It is seen that the scalogramms is a statistical averaged squared distance between particles. Thus, we expected that an analysis of the scalogramms allowed us to find characteristic scales.

Distributions of local minimum and maximum positions in the scalogramms of the events of $S+Em$ interactions at the energy 200 GeV/nucleon are given in Fig. 3. Though there are some irregularities in the distributions, we can not say that they have a statistically guaranteed meaning. In addition, the analysis of connection between a_{min} and a_{max}, and characteristics of the real events did not show any regularity. However, we believe that the study of a larger volume of experimental data will produce interesting results.

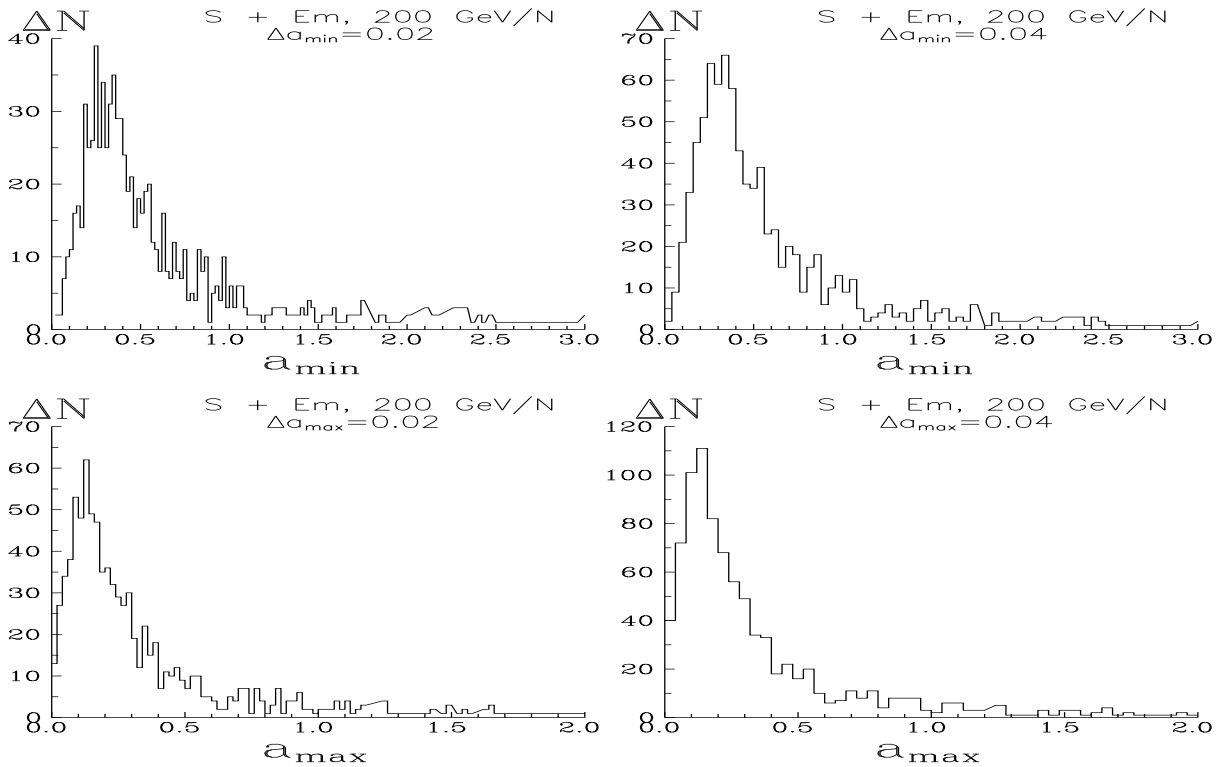

Figure 3: Distributions of the extreme points of the scalogramms of the $S + Em$ events

The next step of our study was search for extremum points of function $W_\Psi(a, b)$ of the real events. Distributions of points on the dilation scale in our interactions are presented in Fig. 4. At the first glance, the distributions have no any characteristic peculiarities – bumps or pits. We only can mark that the distributions can not be described by a simple exponential function. It is necessary to use at least 2 exponents at fitting the distributions. Simulation of *pp*-interactions with the help of the HIJING program [13] has shown that the appearance of the exponent with a larger slope is connected with

production of jets of particles. So, we consider our distributions as a manifestation of jet existence in nucleus-nucleus interactions.

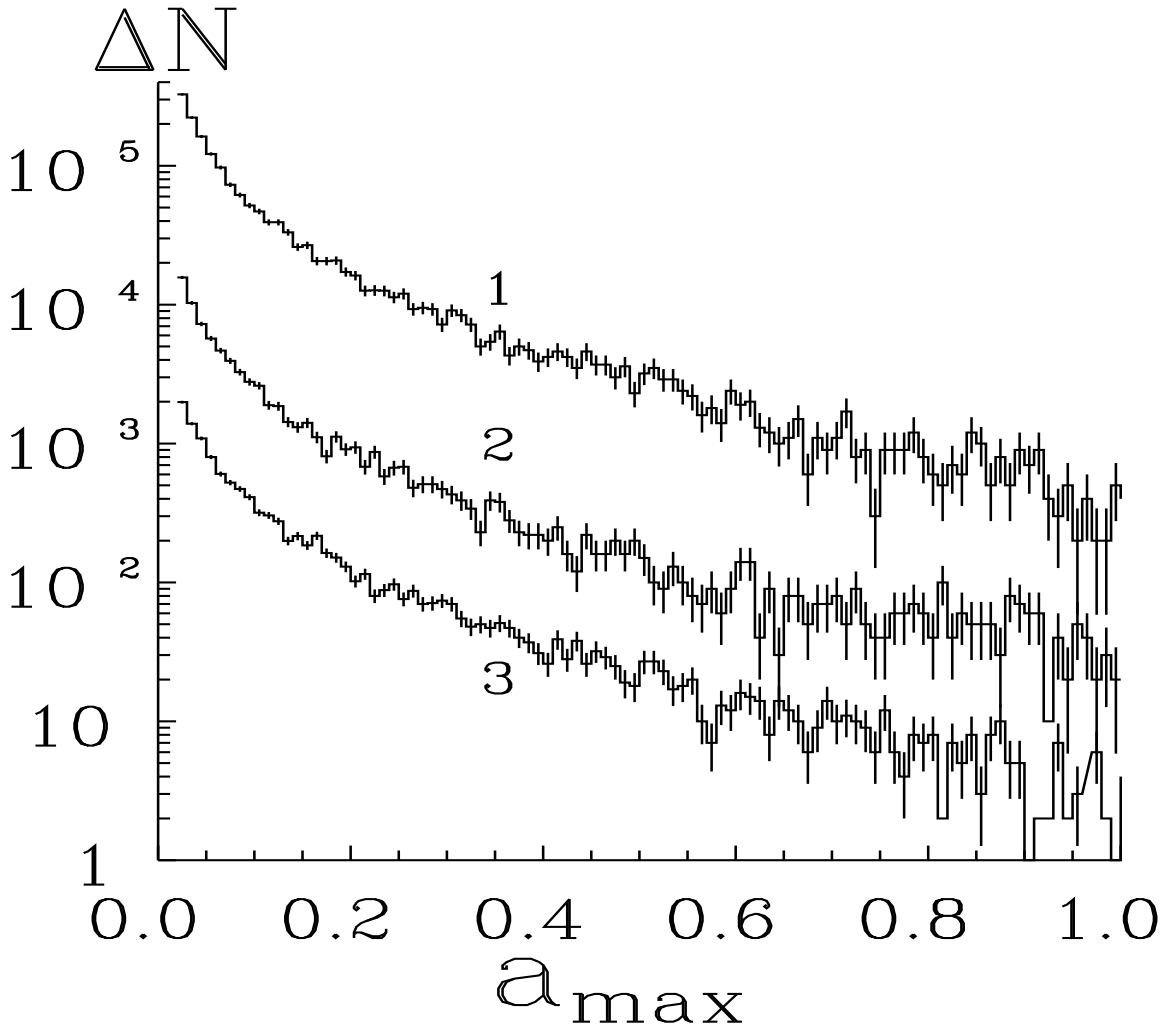

Figure 4: a_{max} distributions in the $S + Em$ and $O + Em$ interactions at the energy of 200 GeV/nucleon, and in the $O + Em$ interactions at the energy of 60 GeV/nucleon (histograms 1, 2 and 3, respectively). The distributions 1, 2, and 3 are multiplied by 10^2, 10^1 and 10^0, respectively.

Research in the distributions of local maximum of $W_\Psi(a, b)$ on b gives more interesting results. The Fig. 4 shows the distributions of all our interactions at $a_{max} > 0.05$ (1), $a_{max} > 0.1$ (2), $a_{max} > 0.2$ (3), and $a_{max} > 0.3$ (4). As seen, the peculiarities of the distributions at $\eta \sim 1.5$, $\eta \sim 2$, $\eta \sim 3$, $\eta \sim 3.5$, $\eta \sim 5$ are located at the same positions for different interactions. The peculiarities, as it can be seen, are connected with narrow groups, where $a_{max} < 0.05$. We interpret them as an existence of preference emission angles of the groups of the particles. Let us note that the positions of some irregularities found by us coincide with those observed early in Ref. [10] at the study of $Pb + Pb$ interactions at the energy of 158 GeV/nucleon. Unlike Ref. [10] where 5 mostly central events were analyzed, we present the results for more than 2000 events.

Research on narrow groups of the particles with help of traditional methods was the third step. Fig. 5 shows a distribution on a pseudorapidity interval between neighboring particles in an event. It was observed that there were pairs of the particles with close pseudorapidities, $\Delta < 10^{-5}$! Their number increases statistical fluctuations. The distribution of the centers of the pairs on η has two bumps at $\eta \sim 3$ and 4. So, we can conclude that the peculiarities of the wavelet spectra observed by us at small scales are connected with the narrow groups of the particles.

One can suppose that such pairs occur due to data input error when two or three entries in the event record are corresponded to the same particle. In this case, such ghost "particles" must have identical η and φ. The fraction of these pairs is lower than 20 % among all the observed narrow pairs. The other pairs have different values of azimuthal angles. The distribution of the particles of the narrow groups on φ (see Fig. 6) has no clear peculiarities and reflects the methodical drawback of the photoemulsion experiments – a poor identification of particles flying perpendicularly to the emulsion plate (at $\varphi \sim 0^o$ and 180^o). The distribution of the azimuthal angle difference of the particles of the narrow group has no irregularities either. So, these pairs can not belong to a jet of particles. The nature of such pairs is not clear for us.

Summary

1. The continuous wavelet transform has been used for the analysis of more than 2000 events of nucleus-nucleus interactions at high energies ($S + Em$ and $O + Em$ interactions at the energies of 200 and 60 GeV/nucleon).

2. It is shown that the maxima of $W_\Psi(a, b)$ obtained with the help of the g_2 wavelet are associated with the groups of particles.

3. It has been found that the distribution of the group of particles on scales in the interactions under the study is geterogeneous what can be caused by jet production.

4. It is observed that the distributions of the groups on pseudorapidities have irregularities, there are preferences of emission angles of the groups.

5. The pairs of particles with close pseudorapidities, $\Delta < 10^{-5}$, are found for the first time.

The nature of the peculiarities observed by us is not clear yet.

The authors are grateful to the members of the EMU-01 collaboration for their kind permission to employ the experimental data analyzed in this paper. One of the authors (V.V.U.) thanks RFBR (grand N 00-01-00307) and INTAS (grand N 00-00366) for their financial support.

References

[1] H. Weng, K.-M. Lau// J. Atmos. Sci., 1994, **51**, p. 2523

[2] P. Kumar, E. Foufoula-Georgio// Rev. of Geophys., 1997, v. **235**, p. 385.

[3] N.M. Astafyeva, G.A. Bazilevskaya// Phys. and. Chem. of the Earth, 1999, v. **C25**, p. 129.

[4] K. Kudela et al.// Solar Phys., 2001, v. **199**, p. 200.

[5] .. // , 2000, . **170**, c. 1235.

[6] I. Daubechies – Ten Lectures on Wavelets// Soc. for Ind. and Appl. Math., Philadelphia, Pa., 1992, p. 357.

[7] N. Suzuki, M. Biyaima, A. Oksawa// Prog. Theor. Phys., 1995, v. **94**, p. 91.

[8] D. Huang// Phys. Rev., 1997, v. **D56**, p. 3961.

[9] Z. Huang, I. Sarcevic, R. Thews, X.-N. Wang// Phys. Rev., 1996, v. **D54**, p. 750.

[10] N.M. Astafyeva, I.M. Dremin, K.A. Kotelnikov// Mod. Phys. Lett., 1997, v. **A12**, p. 1185;
I.M. Dremin et al.// hep-ph/0007060, 2000;
I.M.Dremin et al.// Phys. Lett., 2001, v. **B499**, p. 97.

[11] M.L. Kopytine et al.// nucl-ex/0104002, 2001.

[12] C. Torrence, G.P. Compo// Bull. Amer. Meteorol. Society, 1998, v. **79**, p. 61.

[13] M. Gyulassy, M. Plumer// Phys. Lett. B, 1990, v. **243**, p. 432;
X.-N. Wang, M. Gyulassy// Phys. Rev. C, 1991, v. **44**, p. 3501.

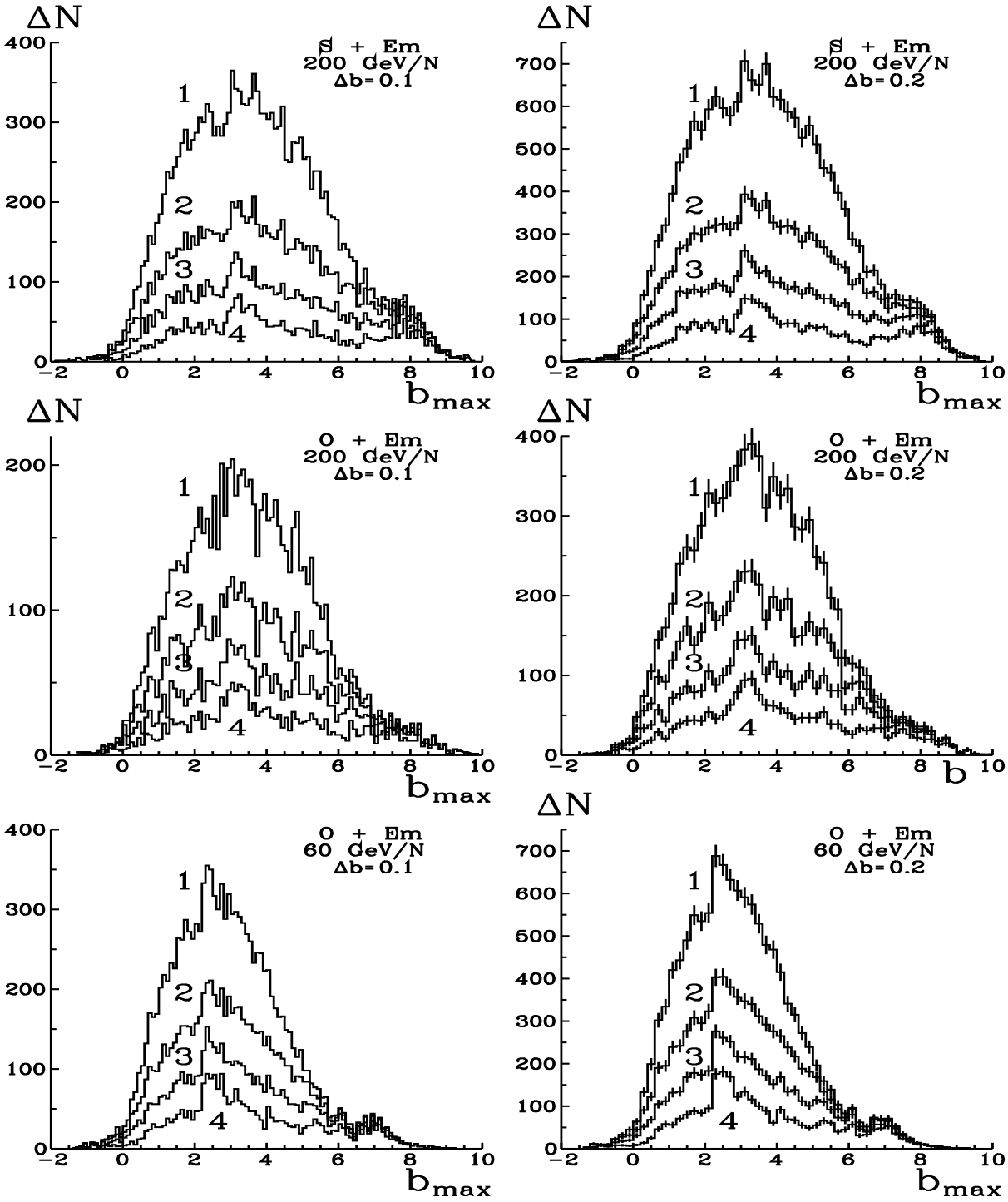

Figure 5: b_{max} distributions in the $S + Em$ and $O + Em$ interactions at the energy of 200 GeV/nucleon, and in the $O + Em$ interactions at the energy of 60 GeV/nucleon. Δb is step of the histogramming. The distributions 1 – 4 are obtained at $a_{max} \geq 0$, $a_{max} \geq 0.05$, $a_{max} \geq 0.1$ and $a_{max} \geq 0.2$, respectively.

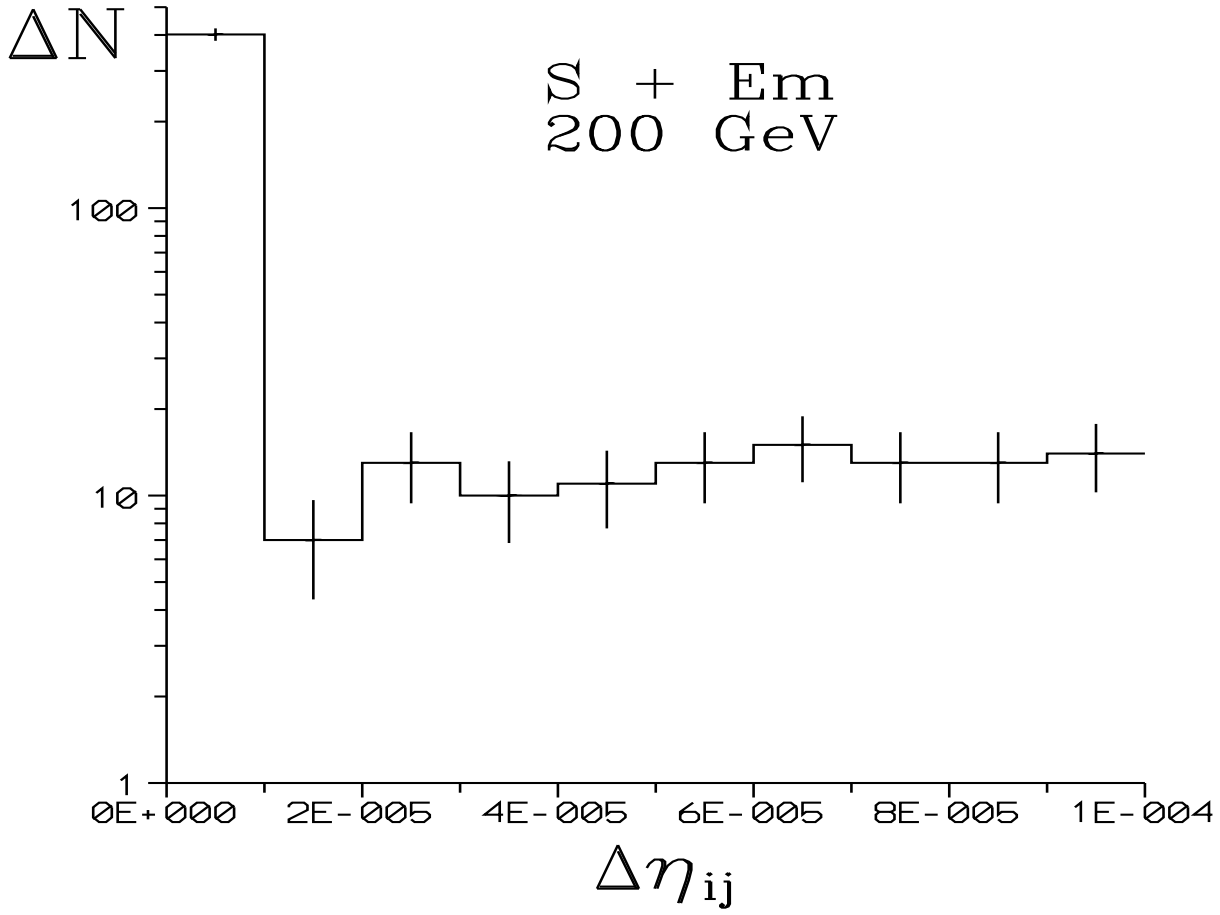

Figure 6: Distribution on the pseudorapidity interval between the neighbouring particles in all studied interactions.

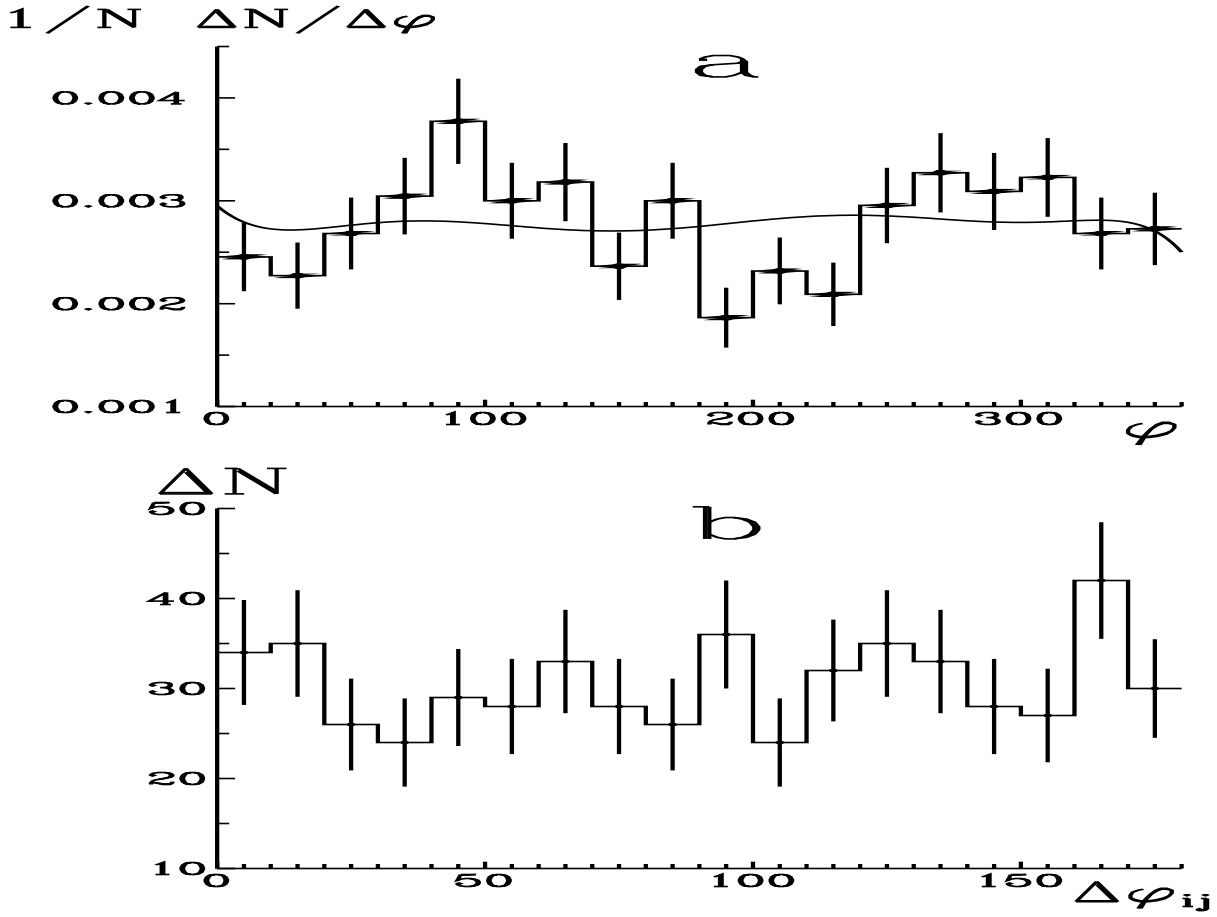

Figure 7: a) The azimuthal angle distribution of particles with close pseudorapidities. The distribution of all particles is presented by solid line. b) The distribution on the azimuthal angles difference of particles with close pseudorapidities.